International Journal of Materials Science ISSN 0973-4589 Volume 12, Number 2 (2017)

MODELING AND SIMULATION FOR WELDING OF AISI 316L STAINLESS STEELS USING PULSED Nd: YAG LASER

A. Jayanthi * [a, b], K. Venkatramanan [c], K. Suresh Kumar [d]

[a] Research Scholar, Department of Physics, SCSVMV university, India
[b] Department of Physics, Jeppiaar Institute of Technology, Chennai, India
[c] Department of Physics, SCSVMV University, India
[d] P.T. Lee Chengalvaraya Naicker College of Engineering, Kanchipuram, India
**E-mail: lectsuresh25@gmail.com*

ABSTRACT

A model was developed for AISI 316L stainless steel welding using a pulsed laser beam as heat source with help of COMSOL multiphysics. The thermal profiles estimated in terms of surface temperature and isothermal contour, hence, the temperature distribution was probed at radial directions from centreline weld and on depth direction of the laser spot position were observations and discussed. Similarly, the thermal profile of the keyhole was predicted when pulse presence and absence, the shape of the keyhole was viewed from top and front view. The predicted keyhole was compared with practical observation and the results are justified. Temperature depended change in non-linear physical properties such as density, thermal conductivity, thermal diffusivity, total enthalpy, inward heat flux and Paclet number are plotted for welding of AISI 316 L stainless steel joint in order to study the change in microstructure and hence the mechanical properties.

Keywords: Autogenous welding, pulsed laser, modeling, stainless steel, temperature distribution, thermal profile.

1.1 INTRODUCTION

Simulation of any physical processes gain most importance both for manufacturing and to enable thorough understanding. As per as, laser welding is concern, it is not yet a state of the art due to the complexity of process parameters. Usually, laser welding process requires correct value of operating parameters to ensure successful weld joints. Hence, a simulation prior to laser welding processes are of major importance to modern industrial demanding without cost penalty in a short span of time [1].

Many authors have done the modeling through differential equations based on control volume method to evaluate the thermal and its related process during various welding techniques. It was briefed about the history of most welding and related processes are modeled using numerical methods and several codes have been developed in order to simulate variety of materials processing including laser welding was briefed up to date **[N1].** Newly developed multi physics software's like LUMET (for laser ultrasonic metallurgy), open FOAM and COSMOL are allow us to simulate the texture of the sample, grain size and growth temperature of the austenite phase in steels, including keyhole oscillations during laser welding process [2]. It has been compiled numurous models which are successfully simulated for different welding process for various combinations of materials [3].

An insight gained from [3-10], it has decided to develop a model for AISI 316L stainless steel (2 mm thick sheets) weld joint using pulsed laser using COMSOL multiphysics code. The temperature depended physical properties such as density, thermal conductivity, thermal diffusivity, total enthalpy and inward heat flux are plotted for welding process in order to manipulate the microstructure and thermomechanical properties of the joint in postweld processing.

2.1 PHYSICS OF HEAT CONDUCTION DURING WELDING PROCESS

In this model, we intended to determine the temperature distributions across weldment in either side of the centreline while it is exposed to a moving laser beam during welding with known parameters. Thus, the heat conduction principle is considered and solved as the main physics for this problem. The speed of heat conduction depends on the material density, specific heat capacity and thermal conductivity, the difference in temperatures, and the shape of the conductor in principle. Hence, the time dependent heat conduction equation is given by

$$\rho c_p \frac{\partial T}{\partial t} + \rho C_p U \nabla T = \nabla(K \nabla T) + \text{----- (1)}$$

Boundary condition for thermal insulation

$$-n.(-K\nabla T) = 0 \text{----- (2)}$$

Since, it is an autogeneous weld, no filler materials were used. The assumptions made relevant to this model is refered from [11].

2.2 MODEL DEFINITIONS

AISI 316L stainless steel sheets having 40 mm (length) x 10 mm (breadth) x 2 mm (thick) are modeled as a butt joint position. The wavelength, focused waist diameter (spot diameter), average peak power density (APPD) and translational velocity of pulsed Nd: YAG laser are given in table 1. The distance to be moved in a translational velocity of 3mm/s along y-axis to reach entire joint along the weldline starting from point (10, 3, 1) as shown in Figure 1. The heat loss is via radiation to the ambient temperature is assumed to be an initial value fixed as 293K.

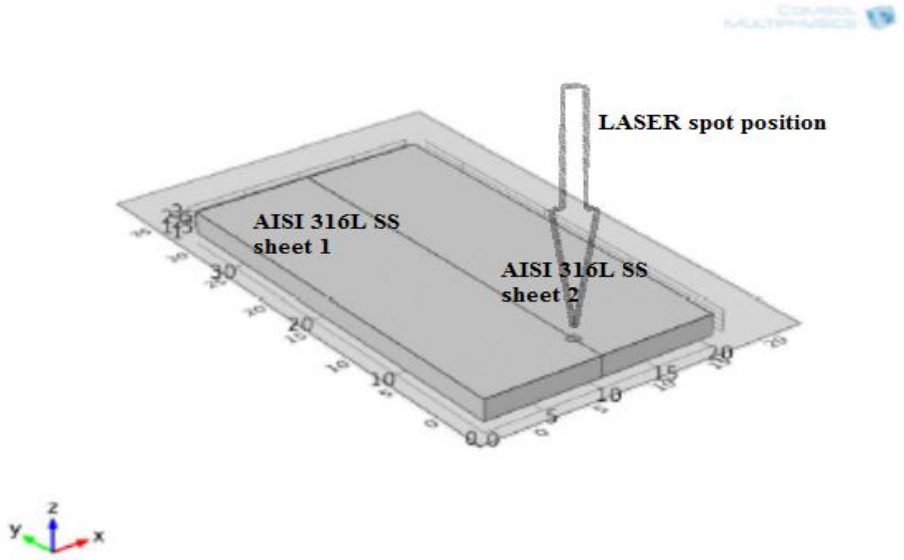

Figure1: The model of AISI 316L stainless steel (2 mm thick) on work plane

Here, laser is considered as a Hermit-Gaussian pulse spatially distributed Transverse Electro Magnetic (TEM_{00}) mode heat source. Because, TEM_{00} quality laser beam is mostly used for welding, drilling and cutting applications. The global parameters used in this model are given table 2. Typically, Triangular/Rectangular shaped laser pulses are chosen for welding, whereas sine waves are low avarage power density which is suitable heat treatments, cladding and alloying. Now, we chosen the triangular pulse plotted at the pulse duration (P_D) 12 ms as shown in figure 2. The focal

point is targeted to irradiate with the sequences of pulses to define its position along the Y-axis over required simulation time. The mesh model for AISI 316L stainless steel joint having dimensions 2 mm (Z-thickness) X 10 mm (X-width) and 40 mm (Y-breadth) is plotted with the governing heat transfer equation at the tolerance about 1 µm as shown in figure 3. The development of 316L stainless steel weld geometry, laser beam profile, pulse shape and the mesh models are established by the procedures adopted as discussed in [3].

Table 1: The Nd: YAG laser specifications for this model

S.No	Specifications	Values	Units
1	Wavelength (λ)	1.064	µm
2	Spot diameter (d)	0.451	µm
3	Average peak power density (APPD)	2000	Watts
4	Welding velocity (U)	3	m/s
5	Pulse duration (P_D)	12	ms

Table 2: Global parameters for modeling and simulation process

Name	**Expression**	**Description**
x_0 Pulse	10[mm]	center x-coordinate
y_0 Pulse	3[mm]	center y-ccordinate
z	1 [mm]	1-3 mm (2mm thick) on butt joint
sigx	0.225[mm]	Pulse x standard deviation
sigy	0.225[mm]	Pulse y standard deviation
Q_0	2100[W]	Total laser power
L_1	10[mm]	Sheet size 1
L_2	10[mm]	Sheet size 2
L_z	2[mm]	Sheet thickness
pulse_width	12[ms]	Temporal pulse width
time_step	pulse_width/5	Time step to store solution
end_time	5[s]	Last time step

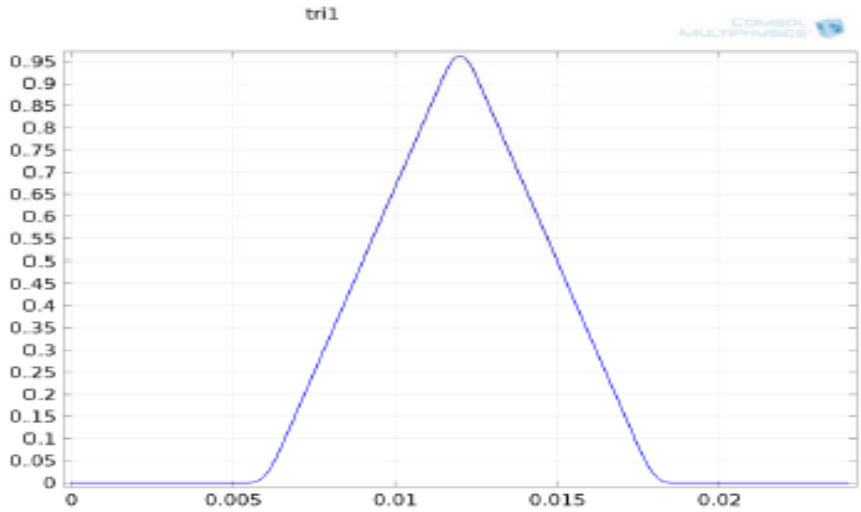

Figure 2: Triangular pulses define its shape for the pulse duration 12 ms

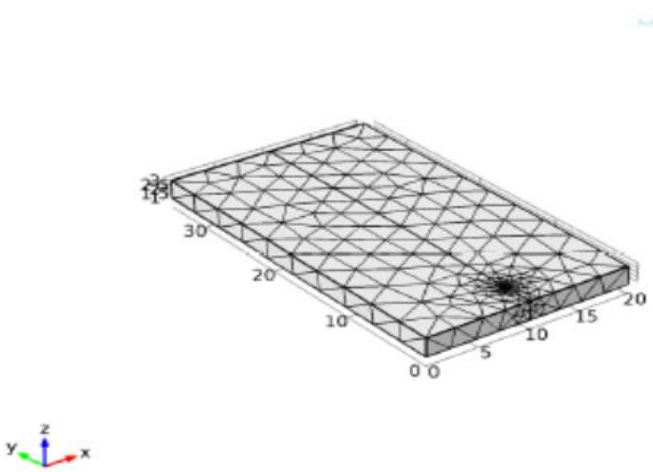

Figure 3: Mesh modeling of AISI 316L stainless steel joint

RESULTS AND DISCUSSIONS

3. THERMAL PROFILE OF PULSED LASER WELDING

The model has developed with all the required parameters and simulated for the processing time step for 5 sec.The average isosurface temperature and the thermal contours across AISI 316 L stainless steel joint was obtained as output to estimate the temperature distribution during pulsed laser irradiation similar to that of welding process for specified parameters as mentioned above in the model definition. Then, in order to probe temperature distribution in the direction of laser irradiation (z - axis) and across the weldjoint (x – axis), the probe points are considered as as refered in [11]. Fromthose probe points the transient thermal responses in those two coordinates are probed at various points and taken for the discussion. The probed temperature distribution in the direction of laser irradiation and across the weldjoint are recorded and plotted in the form of graphs as shown in figure 5 and 6.

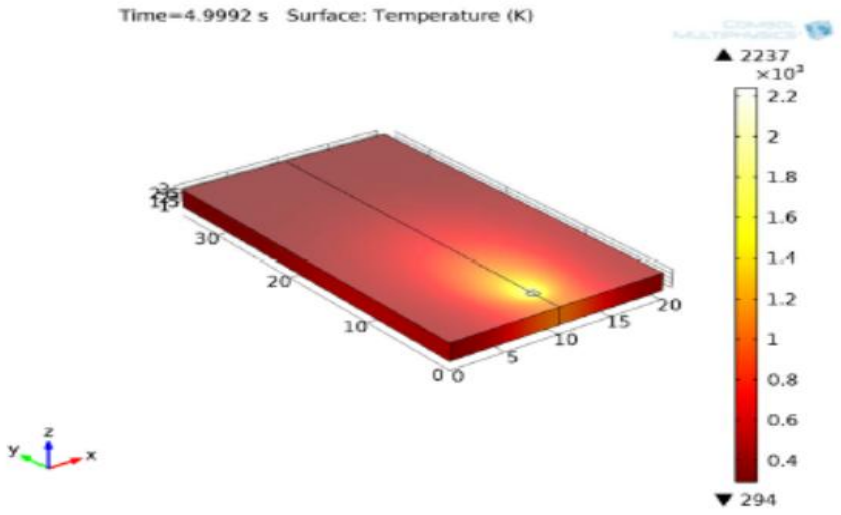

(a)

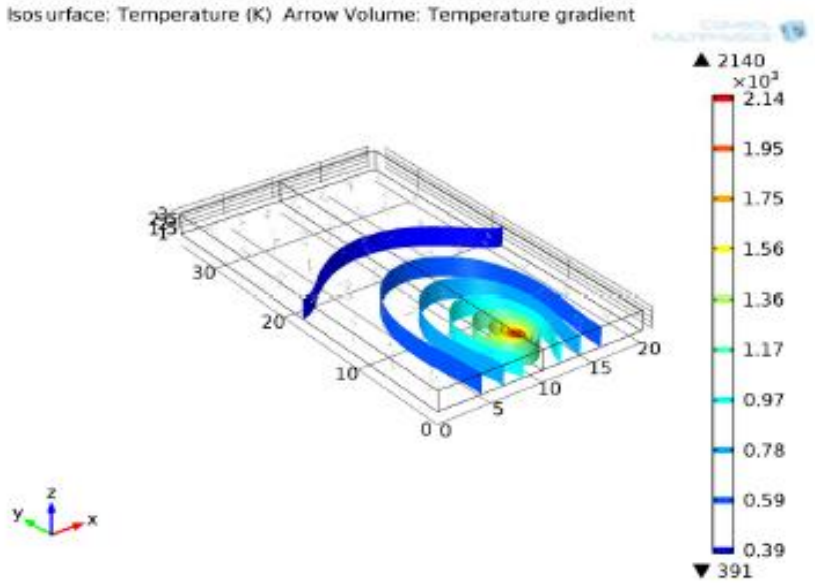

(b)

Figure 4: (a) Temperature distribution in terms of average surface temperature and (b) thermal contours in terms of average isosurface temperature of AISI 316 L stainless steel

Figure 4 is an indication of the capability of present model to perform a successful prediction of temperature ditribution of different regions such as keyhole, melt pool and heat affected zone in a weld joint. Estimation of temperature depended thermo physical properties of these regions are mostly concerned to find its effects on the changes on the microstructure and its consequent changes in mechanical properties due to heat transfer and fluid flow. Since, the thermal profiles obtained from surface temperature and thermal contours directly expose the temperature distribution of entire weld joint. Then, it will be an easier to correlate between temperature distribution and microstructure across joint. In the following discussion, it is interesting to see that how the transient thermal responses probed and justified across the weld joint processed by pulsed laser welding process as shown in figure 4.

3.1 TEMPERATURE DISTRIBUTION IN TRANSVERSE DIRECTIONS FROM WELD JOINT

The locations of the probe points to measure the temperature distributions are chosen across weld joint of AISI 316 L stainless steel as mentioned in figure 5. With respect to the probe points, the transient thermal responses are plotted in terms of average surface temperature across weld joint are plotted and recorded in the form of graphs from (a) to (j) as shown in figure 5. It was noticed that transient temperature distribution start to elevate in the transverse directions (x - axis) while the energetic laser pulses begins to irradiate on top of the butt joint along centreline weld i.e., in y -axis. The graphs (e), (f) and (g) the transient temperature profile appeared with high fluctuations near weldline since the probe points located in and around the region of laser spot. Those peaks in the fluctuations are happened due to the pulsed irradiation of laser and the downfall due to the restoration time interval between the pulses. Further away from those in radial diractions on both sides observed very lesser heat fluctuation in graph (d) and (h) and vanish in graphs (b), (c), and (i) where there is no direct irradiation takes place. However, no melting takes place due to temperature are lessthan that of melting point of the 316L stainless steel (1703K).

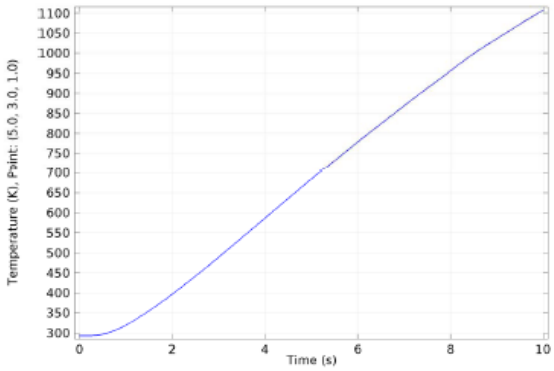

(a) X= 5 mm,Y=3 mm, Z = 1 mm

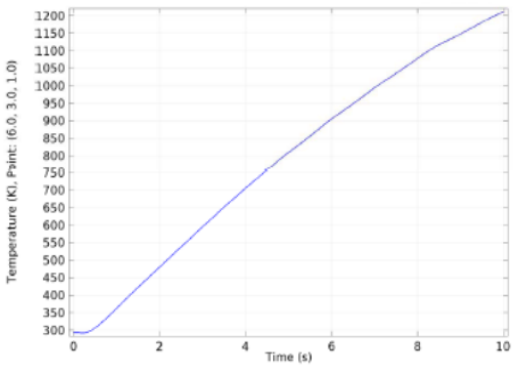

(b) X= 6 mm,Y=3 mm, Z = 1 mm

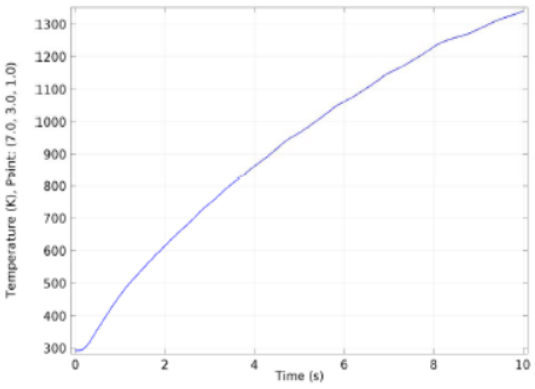

(c) X= 7 mm,Y=3 mm, Z = 1 mm

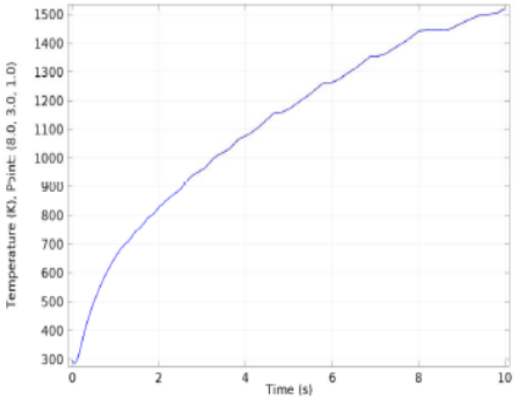

(d) X= 8 mm,Y=3 mm, Z = 1 mm

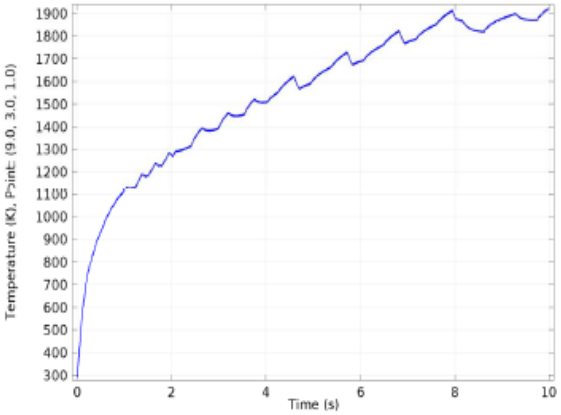

(e) X= 9 mm,Y=3 mm, Z = 1 mm

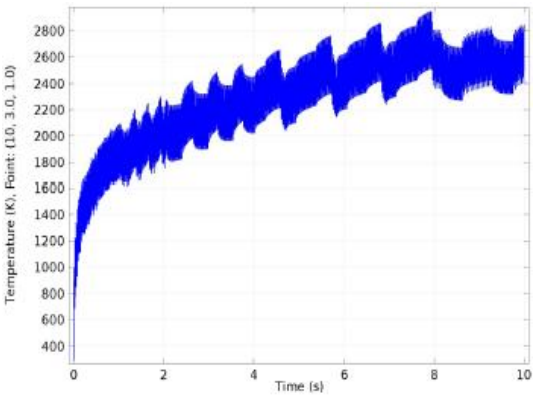

(f) X= 10 mm,Y=3 mm, Z = 1 mm

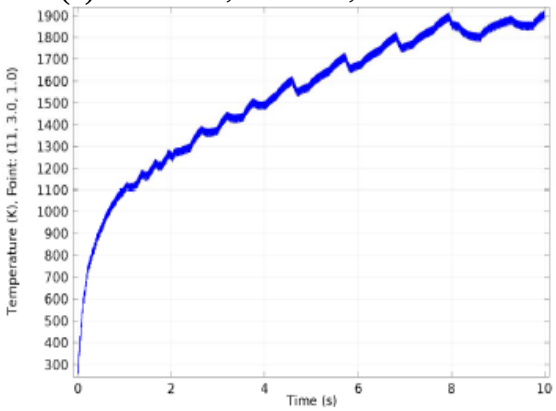

(g) X= 11 mm,Y=3 mm, Z = 1 mm

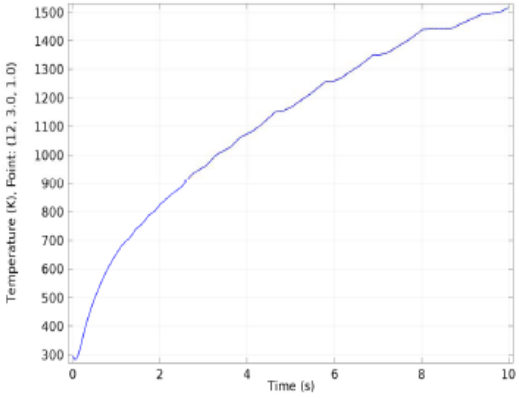

(h) X= 12 mm,Y=3 mm, Z = 1 mm

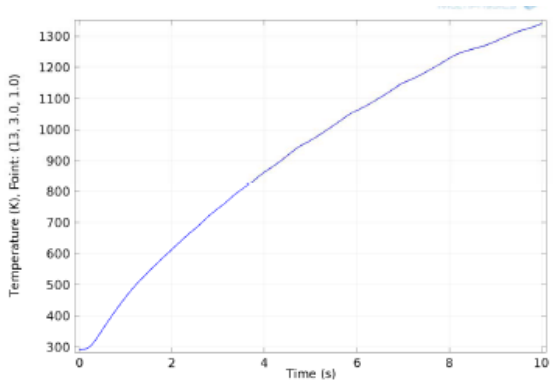

(i) X= 13 mm,Y=3 mm, Z = 1 mm

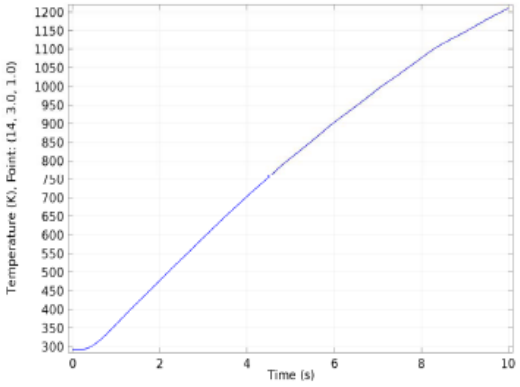

(j) X= 14 mm,Y=3 mm, Z = 1 mm

Figure 5: Calculated Temperature distribution in identified probe points from butt joint welding

The fluctuations completely reduced further in radial distances because of exhibition of parent material for high resistance to heat. In practical, it was observed in weldjoint that the melt pool region and the heat affected zone is limited to very few millimetres in pulsed Nd:YAG laser welding. Thus, estimated temperature distribution are lessthan that of the melting point of 316L stainless steel and only 3 mm of melt zone (e), (f) and (g) observed from the probe points in the radial direction of joint reveals the experimental observations. The temperature is increased linearly as shown in graphs (a) and (j) when the heat is propagated via thermal conduction by free electrons and phonons, subsequently, temperature reaches to thermal balance with ambience condition and the laser irradiation does not have any practical effect further beyond heat affected zone. Thus, one could clearly understand that temperature is spontaneously increased in the region near weldline and decreased gradually around the weldline region towards heat affected zone during welding.

3.2 TEMPERATURE DISTRIBUTION IN THE DIRECTION OF LASER IRRADIATION

There are measuring probe points along the direction of laser pulse irradiation (z – axis) from the top surface for every 0.4 mm upto 2 mm thick and plotted as shown in figure 6. Unlike, radial transmission, the temperature distribution is non-linear in the depth direction. where there is direct interaction between laser and material, the sub surface layers receice and transmits heat energy by various phenomenons such as absorption, heat conduction, melt dynamics, vapour dynamics and phase transition due to the changes occurs in density and refractive index. The high magnitude of fluctuation observed from the top region and it is decreasing towards the end (refer the plots from a - f), this difference of fluctuation between the probe points are due to the temperature gradient occurs in function of thickness (Z – axis) i.e., far from the point of laser irradiation and conduction loss towards the radial directions. These plots itself exposes the conical shape of the keyhole which has observed by practice as shown figure 10.

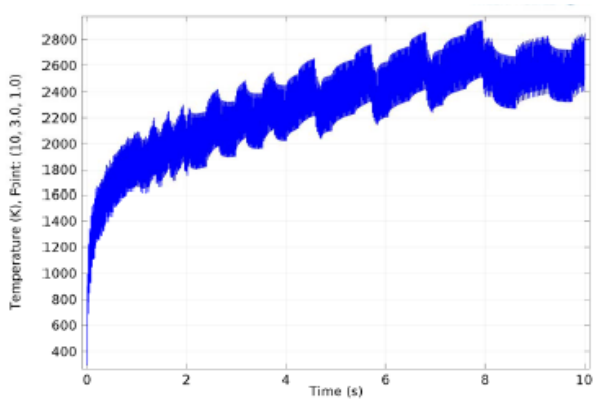

(a) X= 10 mm,Y=3 mm, Z = 1.0 mm

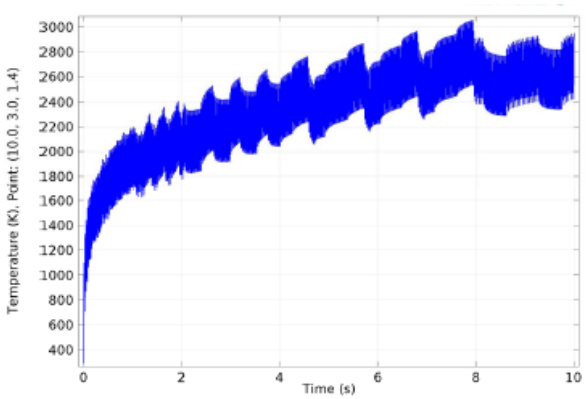

(b) X= 10 mm,Y=3 mm, Z = 1.4 mm

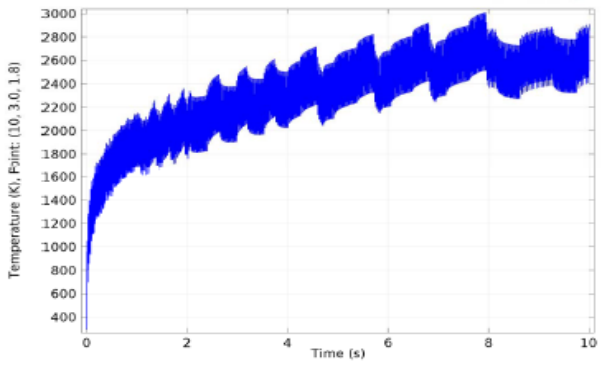

(c) X= 10 mm,Y=3 mm, Z = 1.8 mm

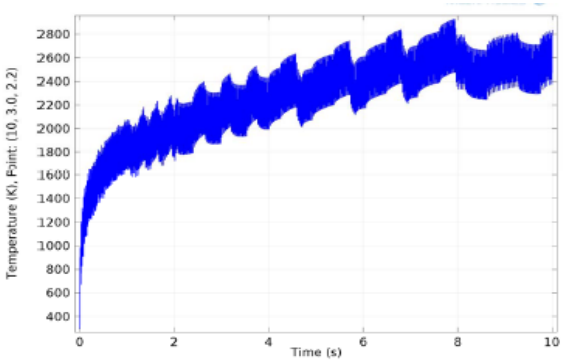

(d) X= 10 mm,Y=3 mm, Z = 2.2 mm

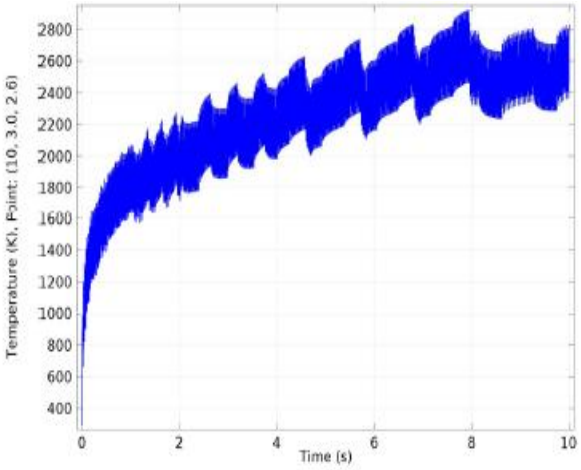

(e) X= 10 mm,Y=3 mm, Z = 2.6 mm

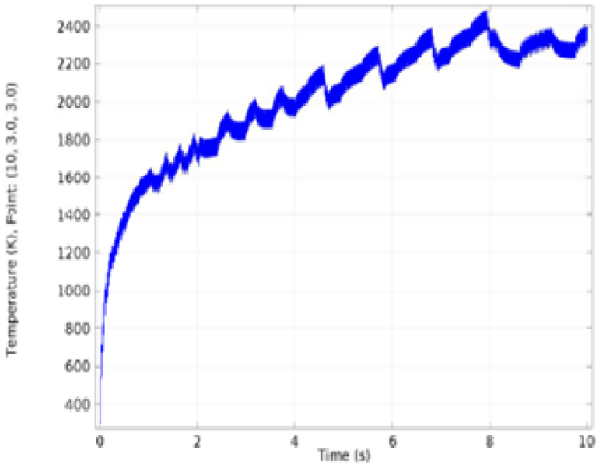

(f) X= 10 mm,Y=3 mm, Z = 3.0 mm

Figure 6: Temperature distribution along depth direction at various probe points

3.3 TEMPERATURE DISTRIBUTION AT THE TOP AND BOTTOM WELD BEAD

Figure 6 shows the time depended temperature distribution in the entire top (plot (a)) and bottom bead (plot (f)) during laser welding. It was noticed that the higer temperature fluctuation throughout the top bead due to the irradiation of pulses and remained well above the melting point of AISI 316 stainless steel. But, the lesser fluctuation observed at the bottom bead because this has has no direct contact with irradiation of pulses and however the temperature always remain well above the melting point which ensure the full penetration welding for entire joint. It's also observed that the peak temperature is not reached simultaneously at the top and bottom but a little delay at the bottom than the top region; it may be due to the various absorption phenomenons are taking place during laser - material interaction. So, it takes some fraction of seconds delay to reach bottom of weld joint than the top. However, both these regions maintain peak temperature above the melting point once it reached and it confirms the full penetration weld throughout which is essential for the joint integrity. However, it is noticed that the transient temperature distribution across the butt joint is symmetric for similar AISI 316L Stainless steel joints and but most of the beam energy transferred to the direction of irradiation rather than its conducts radially as discussed.

3.4 THERMAL PROFILE OF THE KEYHOLE

The specified characteritics of the laser beam and its parameters given in table 1 provides adequate heat flow and its sideways effects increase with pulse duration in terms of the penetration depth [12]. The different stages of laser – material interactions such as conduction, melting, vaporization and even ionization (plasma state) results in a pressure cavity as a deep hole, known as a keyhole. The keyhole has been simulated for AISI 316 L stainless steel joint which has been

plotted in terms of temperature gradient as presented in figure 7. The side view of assumed keyhole structure is appeared wider at the top and shallower at the end (also refer figure 8 (b)). The extended top region of the keyhole in radial directions may exhibit high magnitude conductive and convective heat transfer effectively because of various phenomenons such as Fresnel absorption, thermal conduction, kerr effect, pockel effect, radiation and reabsorption from plasma etc…

This may due to the marangoni flow and buoyancy forces hence the weld surface and fusion zone is appears wider at the top of keyhole. The predicted heat flow directions as arrows in terms of temperature gradient are oriented towards solid region during laser-material interactions (also refer figure 8 (b)) and start decreasing while distance increased. Whereas, the diameter of the keyhole reduced towards the bottom as a function thickness. This may be due to the heat loss by radiation to the ambience, by conduction to the radial directions and larger thermal gradient to the depth. It has also noticed that the thermal gradient is very less in front of the keyhole than behind it as shown figure 7 (b).

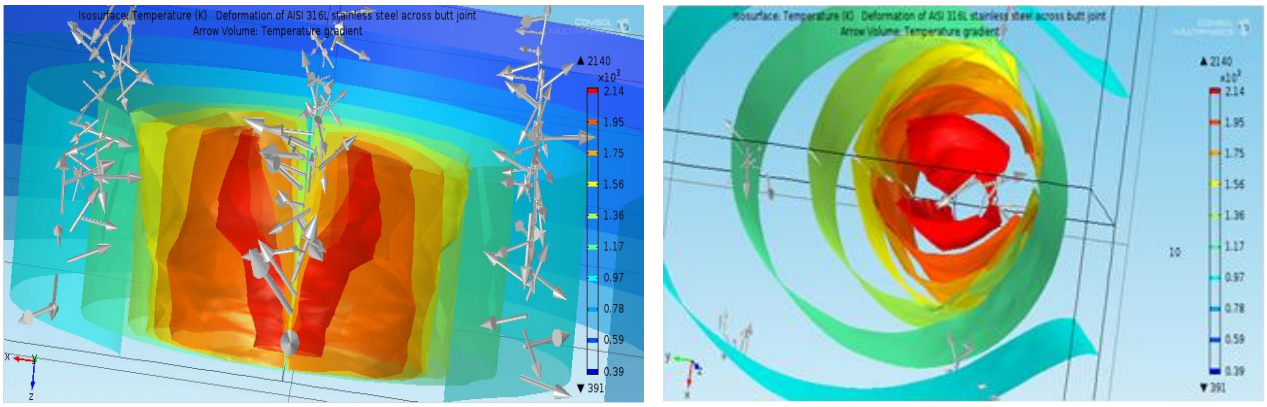

(a) **(b)**

Figure 7: Simulated keyhole profile of AISI 316 L stainless steel in terms of temperature gradient at front view (a) and top view (b).

In a pulsed laser welding, sequences of pulse irradiations plays a major role in an instality of the keyhole geometry. When a new pulse is arrived, the keyhole regain its geometry is regain its shape as we mentioned earlier and arrow directions of transportations of heat flux are oriented outwards from the keyhole as shown in figure 8 (b). When the absence of pulse, geometry of the keyhole become very small since there is no heat input. Now, the heat flux arrow directions are rattled and disoriented. However, heat distribution continues as that of pulse presence, but, a recoil pressure remains to act as a keyhole front which drives the molten material restoration time of a next pulse as shown in figure 8 (a).

In figure 9, the keyhole has been compared at cross sectional view and longitudinal view as obtained from the simulation and experiment. Keyhole is appeared very similar in model and experiment as discussed. The drastic change thermal gradient during restoration between the pulses results in microstructural changes in melt pool in the form of pulse trajectories as shown in figure 9 (a) and (b). The trajectories also reveals the translational motion of laser source at the welding velocity of 3mm/s. The trajectories also reveals the keyhole bent in the opposite direction of welding as observed in figure 8 (b) and 9(b). Thus, this model has been justified the predicted and experimental determination of keyhole during pulsed laser welding of 316L stainless steel.

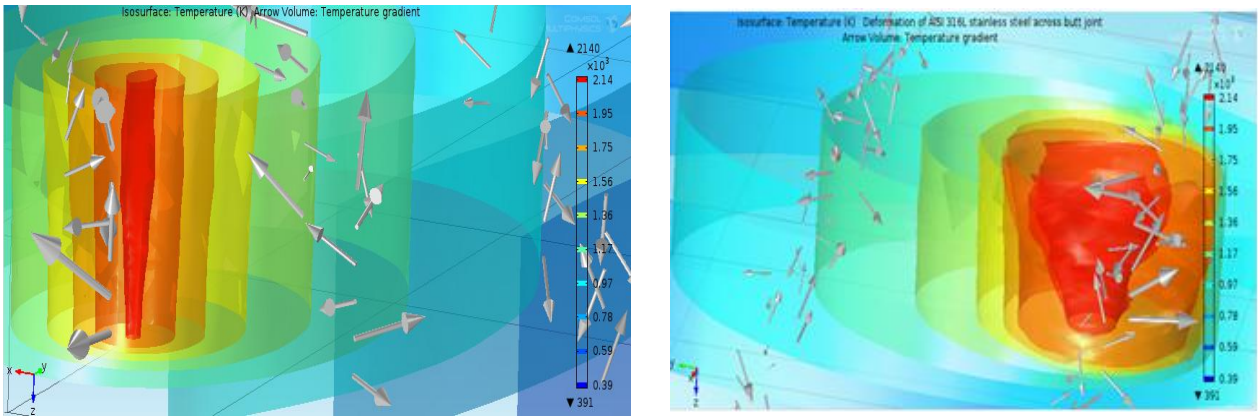

(a) **(b)**

Figure 8: Simulated Keyhole shapes during welding of AISI 316 L stainless steel joint when (a) absence of pulse and (b) presence of pulse.

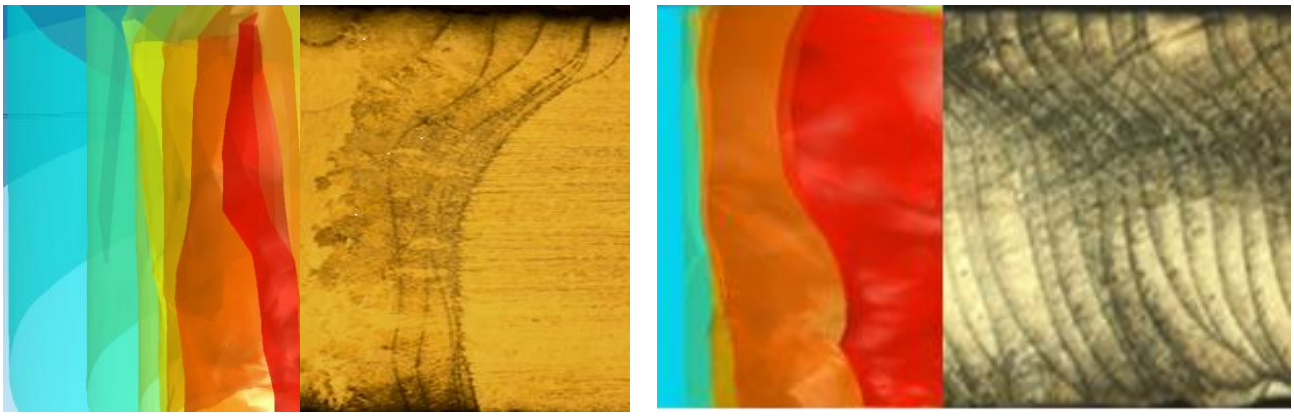

(a) **(b)**

Figure 9: Comparison of keyhole of AISI 316 L stainless steel butt joint between simulation and experimental with (a) cross sectional view and (b) longitudinal view.

3.5 ESTIMATION OF TEMPERATURE DISTRIBUTION IN TERMS OF NON-LINEAR PROPERTIES

The temperature distribution in terms of inward heat flux (a) and Paclet number (b) of the AISI 316L stainless steel joint of the welding process are given as shown in Figure 10. Paclet number helps us to distinguish the solid – liquid boundary [4]. From figure 10, Paclet number is decreasing by an increasing in inward heat flux in and around the laser spot. Its correlate the heat input and Paclet number to distinguish melt region and heat affected zone of entire process.

Similarly, figure 11 shows the non-linear physical properties like density, thermal conductivity, diffusivity and the change in total enthalpy are simulated as functions of transient temperature distribution of 316L stainless steel joint. Estimation of time depended temperature distribution using different probe points among those properties are highly possible using this model as we done in 3.1. Hence, influence of temperature on the changes in microstructure and consequent changes in thermo-mechanical properties are highly predictable using iron-iron carbide diagram, time-temperature transformation diagrams etc... Thus, one can easily predict the heat affected zone, melt pool, penetration depth and keyhole structure of any weldjoint.

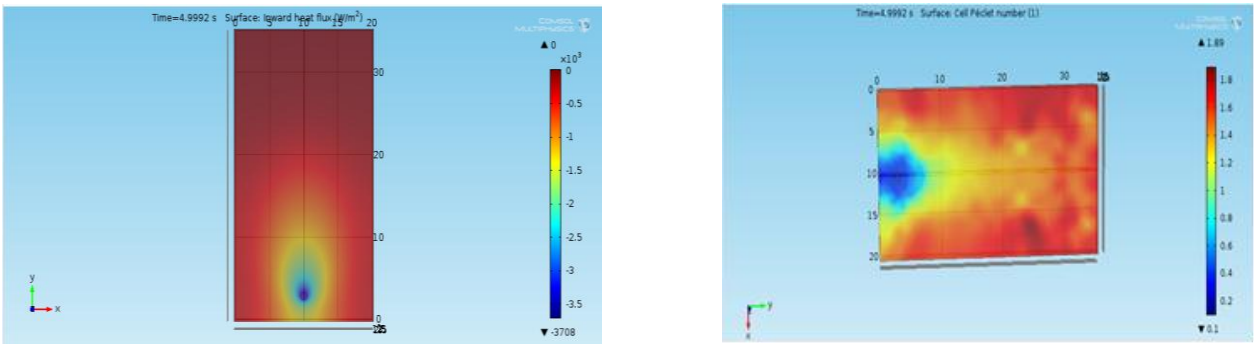

(a) **(b)**

Figure 10: Distribution of temperature in terms of (a) inward heat flux and (b) Paclet number during AISI 316 L stainless steel welding

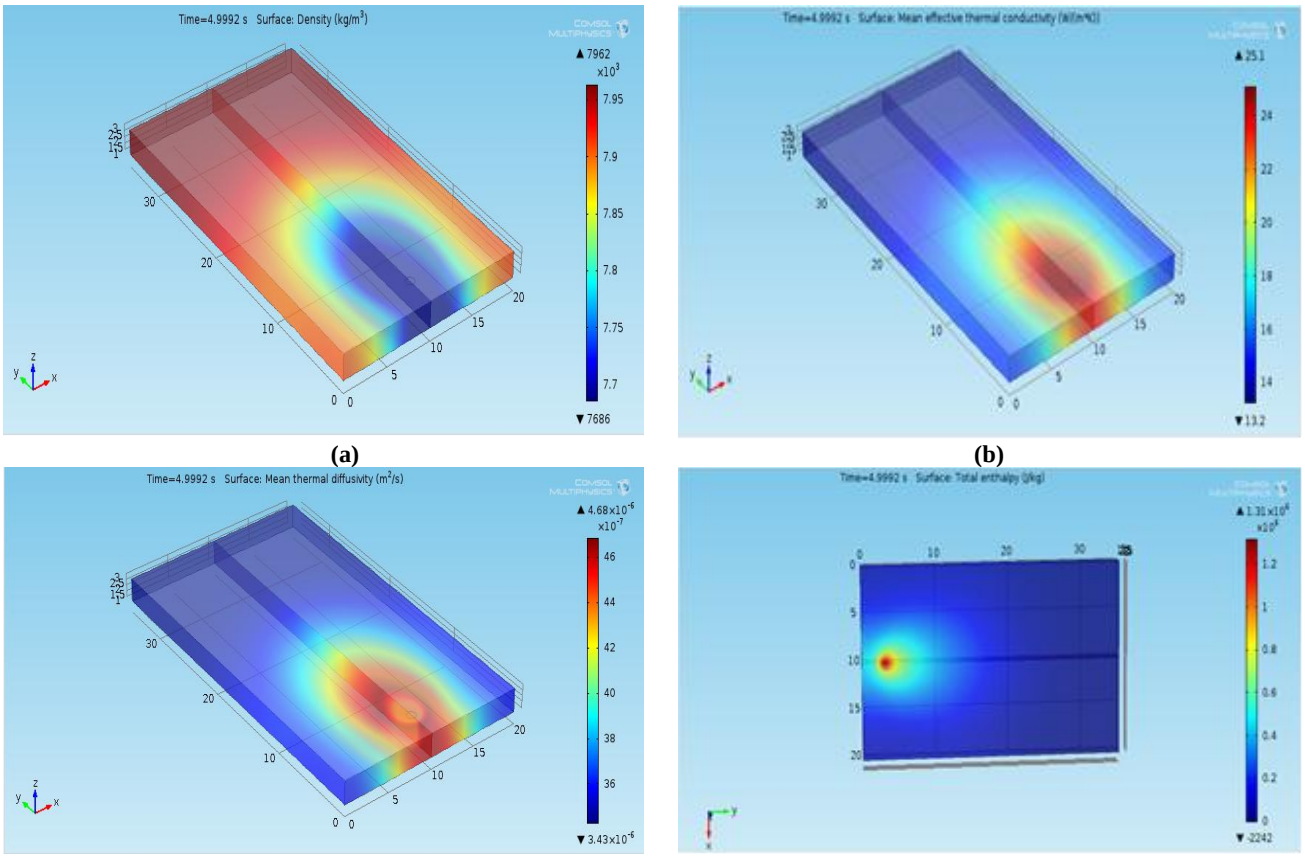

(a) **(b)**

(c) **(d)**

Figure11: Welding of AISI 316L stainless steel simulated in terms of (a) density, (b) thermal conductivity, (c) thermal diffusivity and (d) total enthalpy

4. CONCLUSION

A model was developed for AISI 316L stainless steel welding using a pulsed laser beam as heat source with help of COMSOL multiphysics. The thermal profiles estimated in terms of surface temperature and isothermal contour, hence, the temperature distribution was probed at radial directions from centreline weld and on depth direction of the laser spot position were observations and discussed. Similarly, the thermal profile of the keyhole was predicted when pulse presence and absence, the shape of the keyhole was viewed from top and front view. The predicted keyhole was compared with practical observation and the results are justified. Temperature depended change in

non-linear physical properties such as density, thermal conductivity, thermal diffusivity, total enthalpy, inward heat flux and Paclet number are plotted for welding of AISI 316 L stainless steel joint. Thus, one can easily predict the heat affected zone, melt pool, penetration depth and keyhole structure of any weld joint.

5. REFERENCES

[1] Andreas Otto, Michael Schmidt. LANE 2010: Towards a universal numerical simulation model for laser material processing. Journal of Physics Proceedings, Vol.5, (2010) pp.35-46.

[2] Ferguson D, Chen W, Bonesteel T and Vosburgh J. A look at physical simulation of metallurgical process, past, present and future. Journal of Material Science and Engineering A, Vol. 499 (2009) pp.329-332.

[3] Suresh Kumar K. Numerical modeling of an autogenous butt joint welding of low carbon ferritic steel sheets using a pulsed Nd: YAG laser beam. Indian Journal of Science, 14(43), (2015) pp. 143-150.

[4] Jayanthi A, Venkataramanan K and Suresh Kumar K. A Literature survey on modeling of laser welding and its related processes. IOSR Journal of Applied Physics, Vol.8 (6), (2016), pp. 42-53.

[5] Jayanthi A, Venkataramanan K and Suresh Kumar K. Optimization of operating parameters for autogenous welding of AISI 316L stainless steel and steel using pulsed Nd: YAG laser. IOSR Journal of Applied Physics, Vol.8 (3), (2016), pp. 46-54.

[6] Jayanthi A, Venkataramanan K and Suresh Kumar K. Laser beam a novel tool for welding: A review. IOSR Journal of Applied Physics, Vol.8 (6), (2016), pp. 08-26.

[7] Jayanthi A, Venkataramanan K and Suresh Kumar K. Modeling and analysis of temperature distribution and thermal cycles on a 316Lstainless steel during laser welding. International journal of current science and technology.Vol.4 (5), (2016), pp. 209-215.

[8] Suresh Kumar K. Analytical modeling of temperature distribution, peak temperature, cooling rate and thermal cycles in a solid work piece welded by laser welding process. Procedia Materials Science, Vol. 6, (2014), pp.821 – 834.

[9] Suresh kumar A and Jayanthi A. Modeling of heat and mass transportation in the keyhole of 316L stainless steel and steel joints during pulsed Nd: YAG laser welding. International Journal of Applied Engineering Research. Vol. 10 (22), (2015), pp. 43239-43243.

[10] Jayanthi A, Suresh Kumar K and Venkatramanan K. Selection and Precise Application of Operating Parameters of Nd: YAG and Other Laser Sources for Material Processing. Journal of material science and engineering, Vol. 4, (2015), pp.188. doi:10.4175/2169-0022.1000188.

[11] Suresh Kumar K. Numerical modeling and Simulation of a butt joint welding of AISI 316L stainless steels using a pulsed laser beam. Materials today: Proceedings, Vol. 2(4–5), (2015), pp.2256-2266.

[12] Yih fong Tzeng. Parametric analysis of the pulsed Nd: YAG laser seam welding process. Journal of materials Processing and Technology, Vol.102, (2000) pp.40-47.